Hybrid Deep Pyramid Convolutional Coordinate Attentional Residual Autoencoder Network for Kidney Tumor Diagnosis from CT Scans

Sachin Dattatraya Shingade[1], Midhun Chakkaravarthy[2], Dimitrios A. Karras[3] , Sachin S[4], Komal M Masal[5]
[1]LUCM PetaLing Jaya Malaysia; [2]LUCM PetaLing Jaya Malaysia ; [3] NKUA Athens Greece and EUT Albania;
[4] Zeal COER , Dnyanganga COE, DOT SPPU Pune India ; [5] PICT Pune India
[1]pdf.sachin@lincoln.edu.my ; [2] midhun@lincoln.edu.my; [3] dimitrios.karras@gmail.com;
[4]komalmmasal10@gmail.com ; [5]kmmasal@pict.edu

Abstract: The human kidney is a vital organ responsible for purifying the blood stream by eliminating toxins and metabolic by-products. However, the uncontrolled proliferation of cells can result in tumor formation, presenting with diverse symptoms among individuals. Current methods for kidney tumor classification often struggle with overfitting, high computational complexity, and insufficient accuracy. To address these limitations, a novel deep learning framework has been developed to more precisely identify, measure, and locate tumors within CT scan images, thereby enhancing treatment strategy formulation. Prior to model training, images undergo crucial pre-processing with a Guided Triple Gaussian Functioning Filter , which effectively reduces noise and improves image clarity. Central to this approach is the integration of a Pyramid Convolutional Coordinate Attentional Residual Autoencoder employed for robust semantic feature extraction. This innovative architecture leverages pyramid convolutional layers combined with coordinate attention to accurately focus on tumor-relevant regions within the scans. These refined features are then input into a classification network. This network enhances the learning process by emphasizing both spatial and channel-related information, leading to improved tumor recognition. Additionally, to ensure robust model generalization, the model's hyperparameters are optimally tuned using a Hybrid Spiral Chimp Parrot Optimization Algorithm . The proposed method achieves impressive tumor identification and classification accuracies of 99.7 % and 99.7% respectively, offering substantial benefits for precise oncological diagnosis and therapeutic planning.

Keywords: Kidney Tumor Classification , Medical Image Analysis, CT Scans , Convolutional Neural Networks , Attentional Mechanisms , Residual Autoencoder , Tumor Diagnosis , Treatment .

Introduction

Kidney cancer is a globally prevalent malignancy, and its early detection is crucial for improving patient survival [1]. Renal cell carcinoma (RCC) is the most common type, with clear cell renal cell carcinoma (ccRCC) being its most aggressive variant, accounting for approximately 85% of RCC cases [2]. A concerning characteristic of ccRCC is its propensity to metastasize to distant organs, including the liver, lungs, bones, and lymph nodes [3].

Information technology specialists are actively contributing to kidney disease detection by developing models that simulate renal functions and assist in generating precise diagnostic outputs for healthcare professionals [4]. The advent of extensive medical imaging datasets, coupled with advancements in

machine learning and deep learning techniques, has opened new avenues for research in this domain [5]. Earlier studies explored threshold-based strategies to identify and isolate kidney stones within the renal sinus [6].

Some deep learning frameworks, such as DenseNet, have been utilized for direct tumor detection, bypassing the explicit segmentation stage, and have demonstrated promising accuracy in defining tumor boundaries [7]. However, these models often compromise crucial spatial and structural details, which are vital for practical clinical application. Transfer learning methods have also been employed to enhance tumor prediction by leveraging features from multiple pre-trained models [8].

Related Work

Sasikaladevi et al. [9] presented a CT imaging-based system for detecting prevalent chronic kidney diseases (CKDs), such as stones, cysts, and tumors. Their innovative method involved constructing digital twins from abdominal and urogram CT images. Deep features extracted from these twins were used to build a hypergraph representation of the kidney scans, which were then processed by hypergraph convolutional neural networks to identify significant patterns. The model achieved a high accuracy of 99.71% on a hold-out validation set. Pande et al. [10] introduced a deep learning framework, YOLOV8N-CLS, to aid in diagnosing various renal conditions, specifically addressing the global shortage of urology specialists. Their model classified kidney abnormalities into four categories: cysts, tumors, kidney stones, and normal cases, utilizing data from medical centers in Dhaka. This system, leveraging the advanced capabilities of the YOLOv8 algorithm, demonstrated a robust performance with 82.52% accuracy, 85.76% precision, 75.28% recall, a 75.72% F1 score, and 93.12% specificity for identifying diverse kidney issues.

Pan et al. [11] developed a hybrid detection system for recognizing renal incidentalomas in CT scans, integrating the Swin Transformer with the YOLOv4+ASFF architecture. This framework utilized a backbone network to generate multi-scale feature maps, enabling YOLOv4 to detect targets of varying dimensions. An encoder-decoder structure, incorporating self-attention via a Transformer module, captured long-range dependencies, while Adaptive Spatial Feature Fusion (ASFF) was implemented to manage diverse feature scales. After training for 120 epochs on 990 training and 495 validation images, the model achieved an overall accuracy of 88.2%. Karthikeyan et al. [12] designed a comprehensive CNN-based deep learning model for analyzing kidney disorders using CT scan imagery. They trained their model on a manually labeled dataset of 1,812 cross-sectional CT images, encompassing kidney stones, cysts, and tumors, achieving a 99.17% detection rate during validation. Further validation on a larger dataset (2,283 tumor, 3,709 cyst, 1,377 stone, and 5,077 normal samples) confirmed the model's robustness, yielding a 99% classification accuracy.

Proposed work

This study introduces an advanced deep learning architecture specifically engineered for the precise detection of kidney tumor position, dimensions, and extent, thereby facilitating the planning of subsequent medical treatments. The entire workflow of this proposed system is illustrated in Figure 1, which outlines the sequential stages of a novel multi-scale approach for segmenting kidney tumors.

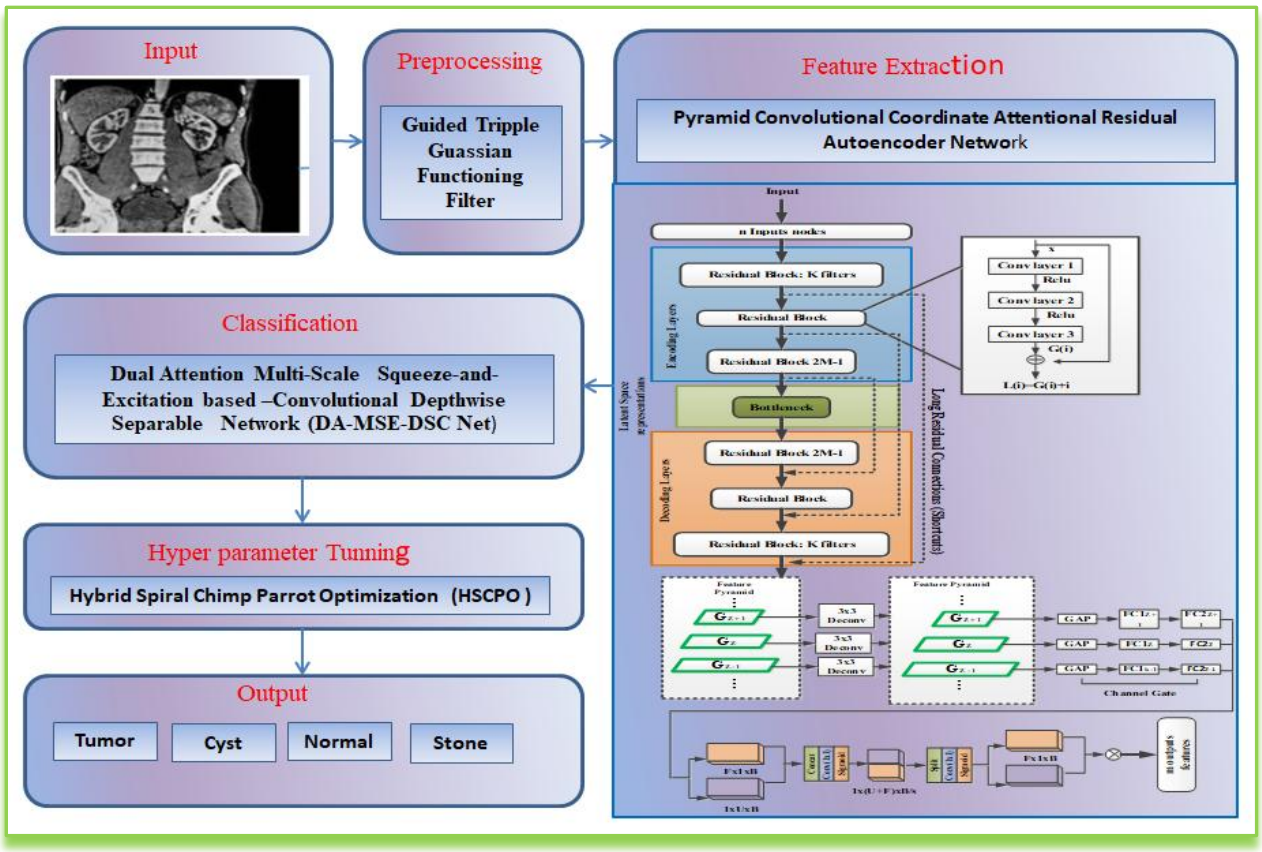

Figure 1. Hybrid Deep Pyramid Convolutional Coordinate Attentional Residual Autoencoder Network Architecture

The process begins with raw input CT images, which first undergo an essential pre-processing step. A Guided Triple Gaussian Functioning Filter (GTGFF) is then applied to these images. This filter effectively eliminates undesirable noise while carefully preserving crucial structural details within the scans, ensuring clearer visual data for subsequent stages. Following pre-processing, significant features are extracted using a Pyramid Convolutional Coordinate Attention-based Residual Autoencoder (PCCARAE). This component harnesses a multi-scale convolutional framework in conjunction with coordinate attention, enabling the model to specifically focus on the most relevant tumor areas. These extracted features are then fed into a Squeeze-and-Excitation-based Dual-Attention Multi-scale Squeeze and Excitation based Convolutional Depthwise Seperable Network (DA-MSE-DSC Net), which performs the accurate classification of the tumor. To further enhance the model's overall performance, its hyperparameters are optimally tuned using a Hybrid Spiral Chimp Parrot Optimization Algorithm (HSCPO). Figure 1 provides a comprehensive visual representation of each stage within this proposed methodology.

Pre-processing

The Guided Triple Gaussian Functioning Filter (GTGFF) is introduced as an advanced pre-processing technique specifically designed to enhance CT scan images, particularly for applications like kidney tumor detection. This filter builds upon the established guided filter framework, which employs a linear

transformation model to derive an output image from an input image and a guided image, typically through window-based averaging to maintain edge integrity. By employing this multi-component Gaussian approach within its filtering operations, GTGFF aims to achieve superior contrast and differentiation between various tissue types. This improved clarity is especially vital in complex anatomical regions like the kidney, enabling clearer visualization of tumor boundaries and differentiation from healthy tissue. The filter's parameters, including mean, standard deviation, and intensity values, are carefully determined to optimize this edge enhancement, ensuring precise information extraction. Ultimately, GTGFF serves as a critical initial step in medical image analysis pipelines, providing high-quality, noise-filtered images essential for accurate downstream tasks like tumor segmentation and classification.

Pyramid Convolutional Coordinate Attentional Residual Autoencoder Network

The presented frameworks architecture is built upon a combination of pyramid-style convolutional attention mechanisms and residual learning blocks, primarily aiming to capture critical spatial and directional features for precise diagnosis. In the initial processing stage, input images undergo transformation through multiple convolutional layers arranged in a pyramid configuration. This hierarchical structure allows the model to extract features at diverse resolutions, thereby enabling it to discern both broad contextual information and fine-grained anatomical details. The pyramid design ensures that features from various levels of abstraction are synergistically combined to form a comprehensive representation of the image content.

Subsequently, these extracted features are processed within a series of residual blocks. The inherent residual connections within these blocks facilitate the learning of deeper, more complex feature representations without succumbing to issues like gradient vanishing. Additionally, integrated attention modules strategically guide the model's focus towards the most relevant spatial regions and critical channel-wise dependencies, improving feature saliency. A unique aspect of this architecture involves generating distinct vertical and horizontal directional information maps. These orientation-specific maps are crucial for discerning subtle edges and patterns, which are vital for accurate tumor localization. This is achieved through the application of specialized 1×k and k×1 convolutional filters, designed to isolate patterns along each axis.

Furthermore, the framework incorporates a cross-level feature fusion strategy, where low-level features (rich in spatial precision) are meticulously combined with high-level features (rich in semantic content). This fusion process ensures that the refined feature representation maintains both accurate localization and contextual understanding. Finally, this unified feature representation is passed through decoding layers to reconstruct the output map, highlighting tumor areas with significantly improved accuracy. Equation (1) represents the final re-calibrated feature map derived from the attention mechanism, specifically from the Coordinate Attention module. This operation scales the original input feature map based on spatially derived attention weights:

$$t_b(x,y) = w_b(x,y) \times k_b^u(i) \times k_b^f(y) \quad (1)$$

t_b(x,y) denotes the final output feature map at spatial coordinates (x,y), which has been enhanced by attention. w_b (x,y) represents the original input feature map at the same coordinates. $k_b^u(i)$ and $k_b^f(y)$ are sets of learned attention weights or coefficients specific to the height (row index i) and width (column index j) dimensions, respectively. These weights are generated by the Coordinate Attention module to quantify the importance of different rows and columns. The element-wise multiplication (×) highlights the presence of the object of interest (e.g., kidney tumor) within specific rows and columns, enabling precise localization and extracting essential feature information. This refined map is then used for subsequent processes like tumor detection.

Kidney Tumor Detection and Classification

Dual Attention Multi-Scale Squeeze-and-Excitation based –Convolutional Depthwise Separable Network (DA-MSE-DSC Net) is employed as the primary classification architecture for kidney tumor detection from medical images. This module receives the refined feature embeddings and performs the ultimate classification, assigning the input image to specific tumor classes. This comprehensive architecture combines efficiency, multi-scale processing, and sophisticated attention mechanisms for robust kidney tumor classification.

Hyperparameter Tuning

The proposed model utilizes the Hybrid Spiral Chimp Parrot Optimization (HSCPO) as its hyperparameter tuning mechanism, aiming to significantly enhance the generalization capabilities of the deep learning architecture. This meta-heuristic approach combines the strengths of two nature-inspired algorithms: the Chimp Optimization Algorithm (ChOA) and the Parrot Optimization (PO) algorithm. This optimization process aims to find the optimal set of hyperparameters that lead to superior model generalization and robust performance in kidney tumor classification.

Results and Discussion

The research was conducted using the Python programming language on a system equipped with an Intel(R) Core(TM) i5-9500 CPU operating at 3.00GHz, a 4GB GPU, and 16GB RAM, running on a 64-bit Windows platform. The proposed deep learning model underwent training for 300 epochs. The Adam optimizer was chosen for its efficiency in handling sparse gradients and adaptive learning rates. Categorical crossentropy was utilized as the loss function, a standard choice for multi-class classification tasks. Both training and validation losses were dynamically calculated and monitored throughout their respective phases. To mitigate the risk of overfitting, a dropout rate of 0.5 was systematically applied, randomly deactivating 50% of neurons during training. The input data to the network was uniformly scaled to an input shape of 448. The network architecture incorporated Conv1D filters of diverse sizes, specifically 16, 24, 32, 64, 96, and 1280, enabling the extraction of multi-scale features. Furthermore, dilation rates of 1, 2, 3, and 4 were employed to effectively expand the receptive field and capture broader contextual information without increasing computational cost. A squeeze-and-excitation ratio of 16 was also implemented, a hyperparameter designed to enhance feature recalibration and further optimize model performance by dynamically emphasizing more informative channels.

Dataset

The research leveraged a distinct dataset for its investigation. The CT Kidney Dataset, encompasses 12,446 unique medical images. These images were meticulously gathered from various hospitals in Dhaka, Bangladesh, via their Picture Archiving and Communication System (PACS). This dataset specifically includes both coronal and axial views derived from contrast and non-contrast abdominal and urogram CT scans. The images are meticulously categorized into four distinct medical conditions: 3,709 cases of cysts, 5,077 instances deemed normal, 1,377 cases involving kidney stones, and 2,283 cases presenting with tumors. Prior to inclusion, each original DICOM scan underwent anonymization to protect patient privacy and was subsequently converted into a lossless JPG format. A rigorous validation process was conducted by both experienced radiologists and medical technologists to ensure data accuracy and integrity.

Performance Evaluation

Assessing the effectiveness of deep learning systems for kidney tumor detection is critically dependent on a range of standard performance indicators. These key metrics include accuracy, precision, F1-score, the Area Under the Receiver Operating Characteristic Curve (AUC-ROC), Dice score, Intersection over Union (IoU), Mean Absolute Error (MAE), and Mean Squared Error (MSE) [13-14]**.** The majority of these indicators are derived directly from the confusion matrix, which provides a detailed breakdown of a model's true and false positive and negative predictions [15-16]. Employing this comprehensive array of metrics is crucial for gaining a thorough understanding of the model's overall performance and its reliability, particularly in sensitive medical applications where diagnostic precision is paramount [17].

The figure 2 (a), (b), (c) displays a performance evaluation of different deep learning models for classifying CT kidney images, using bar graphs to visually represent the Accuracy, Precision, and Recall metrics. (a) Accuracy Graph illustrates the overall correctness of each model's predictions.

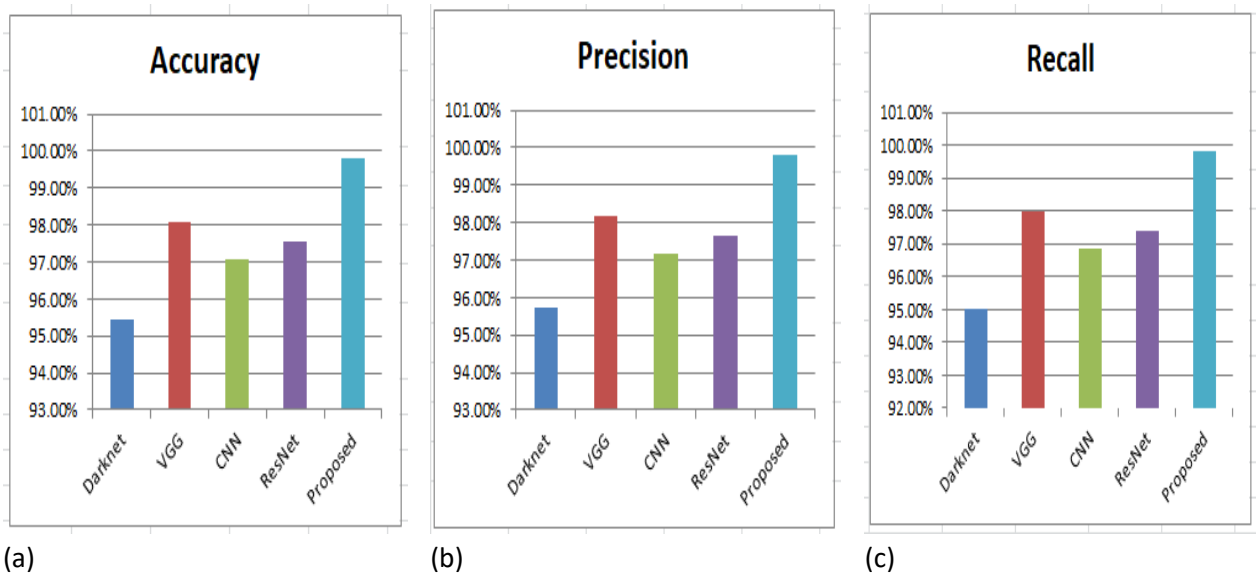

(a) (b) (c)

Figure 2. Performance evaluation (a) Accuracy , (b)Precision , (c)Recall

The "Proposed Model" demonstrates the highest accuracy, achieving approximately 99.71 %, which significantly surpasses other models. In comparison, DarkNet shows the lowest accuracy, just above 95.30%, while VGG performs slightly better at around 98.18 %. Both CNN and ResNet achieve comparable accuracy, hovering around 97%. (b) Precision Graph indicates the proportion of true positive predictions among all positive classifications made by each model. The "Proposed Model" again exhibits the highest precision, registering just over 99.71%. Darknet Net shows the lowest precision, slightly below 95%, whereas VGG and CNN perform better, ranging between 97% and 98%. ResNet's precision is observed to be slightly lower than that of CNN. (c) Recall Graph depicts the proportion of actual positive cases that were correctly identified by each model. The "Proposed Model" consistently leads in recall, achieving approximately 99.71%. DarkNet, VGG, and CNN show similar recall scores, ranging from approximately 95% to 97%, with ResNet performing slightly better than these three.

The figure 3 (d), (e), (f) presents additional performance evaluation metrics : Matthews Correlation Coefficient (MCC), Accuracy for Tumor (%), and Accuracy for Normal (%). for various deep learning models in classifying CT kidney images, displayed through bar graphs. (d) MCC Graph illustrates the MCC score, a more balanced measure for classification quality that considers all four confusion matrix categories (true positives, true negatives, false positives, and false negatives) . The "Proposed Model" achieves the highest MCC, nearing 99.8%, indicating superior overall prediction quality. DarkNet shows the lowest MCC at just above 90.0%, while ResNet, VGG, and CNN fall in between, with VGG slightly outperforming ResNet and CNN. (e) Accuracy (Tumor %) Graph shows the accuracy of each model in correctly identifying "Tumor" cases. The "Proposed Model" achieves the highest accuracy in tumor detection, reaching 99.91%. DarkNet shows the lowest tumor accuracy, below 97%, with VGG performing better around 99%. CNN and ResNet also show strong performance, around 98% for CNN and slightly above 98% for ResNet. (f) Accuracy (Normal %) Graph displays the accuracy of each

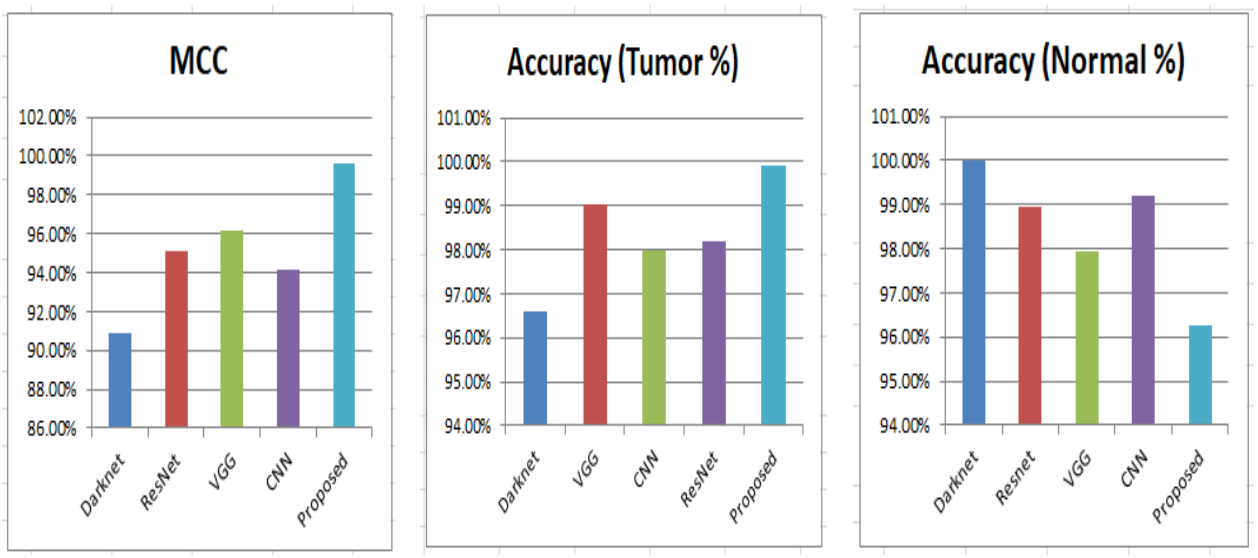

(d) e) (f)

Figure 3. Performance evaluation (d) MCC, (e)Accuracy for Tumor (%), and (f) Accuracy for Normal (%).

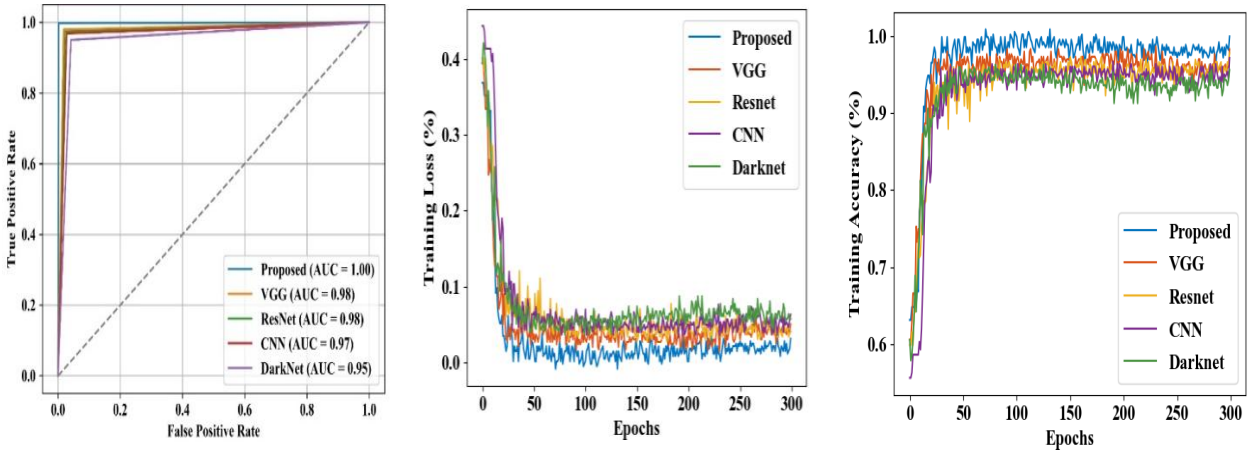

(g) (h) (i)

Figure 4. Performance evaluation (g) ROC Curve Graph, (h) Training Loss Graph , and (i) Training Accuracy Graph.

model in correctly identifying "Normal" cases. DarkNet demonstrates the highest accuracy, at 100%, indicating its strong performance in recognizing healthy tissue. The "Proposed Model" shows the lowest accuracy for normal cases, just above 96%. ResNet, VGG, and CNN perform well, with VGG and CNN both around 98% and ResNet nearing 99.02%. The "Proposed Model" consistently excels in overall Accuracy, Precision, Recall, and specifically in identifying "Tumor" cases, DarkNet shows exceptional accuracy in classifying "Normal" instances.

The figure 4 (g), (h), (i) specifically illustrate the Receiver Operating Characteristic (ROC) curve, Training Loss, and Training Accuracy over epochs. (g) ROC Curve (AUC) Graph , The "Proposed Model" achieves an outstanding AUC of 1.00, indicating perfect discrimination. VGG follows with an AUC of 0.98, while ResNet and CNN both achieve 0.97. DarkNet shows the lowest AUC at 0.95, suggesting it has less discriminatory power compared to the others. (h) Training Loss Graph illustrates how the training loss of each model changes over 300 epochs. Training loss measures the error rate of the model on the training data. A decreasing trend in loss indicates that the model is learning effectively .

The "Proposed Model" demonstrates consistently low training loss throughout the training process, settling at a very low value, which implies efficient learning and convergence. (i) Training Accuracy Graph depicts the training accuracy of each model across 300 epochs. Training accuracy measures the percentage of correct predictions the model makes on the training data. An increasing trend signifies that the model is becoming more proficient at classifying the training examples. The "Proposed Model" reaches and maintains the highest training accuracy, nearing 99%.

Conclusion

The presented research introduces a novel deep learning framework designed to overcome existing limitations in kidney tumor classification, such as overfitting, high computational complexity, and

insufficient accuracy. This innovative solution, incorporating a Hybrid Deep Pyramid Convolutional Coordinate Attentional Residual Autoencoder Network, aims to precisely identify, measure, and locate tumors within CT scan images, thereby enhancing treatment strategy formulation. The experimental results validate the efficacy of this comprehensive framework. The proposed method demonstrates impressive tumor identification and classification accuracies of approximately 99.71% for overall accuracy, precision 99.71 %, and recall 99.71 % , an MCC nearing 99.8% , and a tumor-specific accuracy of 99.91%. Notably, the model achieves an outstanding Area Under the Curve (AUC) of 1.00, indicating perfect discrimination capabilities. Furthermore, the training loss graphs show consistently low values, while training accuracy consistently remains at the highest levels, confirming efficient learning and robust performance on the training data. These metrics consistently highlight the proposed model's superior ability compared to other established deep learning architectures like DarkNet, VGG, CNN, and ResNet. This robust performance offers substantial benefits for precise oncological diagnosis and therapeutic planning in kidney tumor detection.

References

1. Huang, Junjie, David Ka-Wai Leung, Erica On-Ting Chan, Veeleah Lok, Sophia Leung, Iris Wong and Xiang-Qian Lao, "A global trend analysis of kidney cancer incidence and mortality and their associations with smoking, alcohol consumption, and metabolic syndrome." , *European urology focus* 8, no. 1 (2022): 200-209. Doi: doi.org/10.1016/j.euf.2020.12.020.
2. Karunanayake, Nalan, Lin Lu, Hao Yang, Pengfei Geng, Oguz Akin, Helena Furberg, Lawrence H. Schwartz, and Binsheng Zhao. "Dual-Stage AI Model for Enhanced CT Imaging: Precision Segmentation of Kidney and Tumors.", *Tomography* 11, no. 1 (2025): 3. Doi: doi.org/10.3390/tomography11010003
3. Sanders, Christine, Almotasem Salah M. Hamad, Susanna Ng, Racha Hosni, Jörg Ellinger, Niklas Klümper and Manuel Ritter, "CD103+ tissue resident T-lymphocytes accumulate in lung metastases and are correlated with poor prognosis in ccRCC." , *Cancers* 14, no. 6 (2022): 1541. Doi: https://doi.org/10.3390/cancers14061541.
4. Gharaibeh, Maha, Dalia Alzu'bi, Malak Abdullah, Ismail Hmeidi, Mohammad Rustom Al Nasar, Laith Abualigah, and Amir H. Gandomi, "Radiology imaging scans for early diagnosis of kidney tumors: a review of data analytics-based machine learning and deep learning approaches." , *Big Data and Cognitive Computing* 6, no. 1 (2022): 29. Doi: doi.org/10.3390/bdcc6010029
5. Yildirim, Kadir, Pinar Gundogan Bozdag, Muhammed Talo, Ozal Yildirim, Murat Karabatak, and U. Rajendra Acharya, "Deep learning model for automated kidney stone detection using coronal CT images." , *Computers in biology and medicine* 135 (2021): 104569. Doi: doi.org/10.1016/j.compbiomed.2021.104569
6. Cui, Yingpu, Zhaonan Sun, Shuai Ma, Weipeng Liu, Xiangpeng Wang, Xiaodong Zhang and Xiaoying Wang, "Automatic detection and scoring of kidney stones on noncontrast CT images using STONE nephrolithometry: combined deep learning and thresholding methods." , *Molecular Imaging and Biology* 23 (2021): 436-445. Doi: doi.org/10.1007/s11307-020-01554-0

7. Qadir, Abdalbasit Mohammed, and Dana Faiq Abd, "Kidney diseases classification using hybrid transfer-learning densenet201-based and random forest classifier." , *Kurdistan Journal of Applied Research* 7, no. 2 (2022): 131-144. Doi: doi.org/10.24017/Science.2022.2.11
8. Islam, Md Nazmul, Mehedi Hasan, Md Kabir Hossain, Md Golam Rabiul Alam, Md Zia Uddin, and Ahmet Soylu, "Vision transformer and explainable transfer learning models for auto detection of kidney cyst, stone and tumor from CT-radiography." , *Scientific Reports* 12, no. 1 (2022): 11440.Doi: doi.org/10.1038/s41598-022-15634-4
9. Sasikaladevi, N. and A. Revathi, "Digital twin of renal system with CT-radiography for the early diagnosis of chronic kidney diseases." , *Biomedical Signal Processing and Control* 88 (2024): 105632. Doi: doi.org/10.1016/j.bspc.2023.105632
10. Pande, Sagar Dhanraj, and Raghav Agarwal, "Multi-class kidney abnormalities detecting novel system through computed tomography." , *IEEE Access* 12 (2024): 21147-21155. Doi: doi.org/10.1016/j.jrras.2024.100845
11. Pan, Canyu, Jieyun Chen, and Risheng Huang, "Medical image detection and classification of renal incidentalomas based on YOLOv4+ ASFF swin transformer." ,*Journal of Radiation Research and Applied Sciences* 17, no. 2 (2024): 100845.
12. Karthikeyan, V., M. Navin Kishore, and S. Sajin. "End-to-end light-weighted deep-learning model for abnormality classification in kidney CT images." *International Journal of Imaging Systems and Technology* 34, no. 1 (2024): e23022. Doi: doi.org/10.1002/ima.23022
13. Masal, Komal Mahadeo and Shripad Bhatlawande, "An integrated region proposal and spatial information guided convolution network based object recognition for visually impaired persons' indoor assistive navigation." ,*The Imaging Science Journal* 72, no. 7 (2024): 884-897. Doi: http://doi.org/10.1080/13682199.2023.2230419
14. Masal, Komal Mahadeo and Shripad Bhatlawande, "Hybrid Deep Artificial Humming Bird Algorithm For Improved Real Time Blind Assistance with Advanced Jetson Nano GPU.", In *2023 7th International Conference on Electronics, Communication and Aerospace Technology (ICECA)*, pp. 99-104. IEEE, 2023. Doi: 10.1109/ICECA58529.2023.10394801
15. Sachin, D. S., P. M. Rohini, and M. M. Komal. "Random forest machine learning classifier for seed recommendation." In *IEEE-International conference on Edge computing and Applications ICECAA*, pp. 13285-1390. 2022. Doi: 10.1109/ICECAA55415.2022.9936120
16. Shingade, Sachin D., Rohini Prashant Mudhalwadkar, and Komal M. Masal. "Random Forest, DT And SVM Machine Learning Classifiers for Seed with Advanced WSN Sensor Node." In *2022 International Conference on Automation, Computing and Renewable Systems (ICACRS)*, pp. 321-326. IEEE, 2022. Doi: 10.1109/ICACRS55517.2022.10029310
17. Shingade, Sachin D., and Rohini P. Mudhalwadkar. "Hybrid extreme learning machine based bidirectional long short-term memory for crop prediction." *Concurrency and Computation: Practice and Experience* 35, no. 2 (2023): e7482. Doi: http://doi.org/10.1002/cpe.7482